Catalysis Today 150 (2010) 353–357

Contents lists available at ScienceDirect

Catalysis Today

journal homepage: www.elsevier.com/locate/cattod

Photodegradation of phenol and cresol in aqueous medium by using Zn/Al + Fe mixed oxides obtained from layered double hydroxides materials

A. Mantilla [a], F. Tzompantzi [b,*], J.L. Fernández [a], J.A.I. Díaz Góngora [a], R. Gómez [b]

[a] CICATA-IPN, Av. Legaria No 694, México 11500 D.F., Mexico
[b] Universidad Autónoma Metropolitana-Iztapalapa, Departamento de Química, Av. San Rafael Atlixco No 186, México 09340 D.F., Mexico

ARTICLE INFO

Article history:
Available online xxx

Keywords:
ZnAlFe layered double hydroxides
LDHs co-precipitation
Phenol photodegradation
p-Cresol photodegradation
Energy band gap LDHs

ABSTRACT

ZnAlFe layered double hydroxides (LDHs) were synthesized by the co-precipitation method at different M_{II}/M_{III} ratio. The solids were calcined at 723 K obtaining the respective mixed oxides with high specific surface areas (138–70 m^2/g) and semiconductor properties (band gap values of 2.54–2.04 eV). The photocatalytic activity of these materials was tested for the photodegradation of aqueous solutions containing phenol and *p*-cresol (40 ppm), in presence of a UV light source. A disappearance of 98% of phenol and a total photodegradation of *p*-cresol were obtained after 6 and 4 h, respectively.

1. Introduction

Due to increasing water demands and/or long periods of drought, removing pollutants from industrial wastewaters is becoming an important area of research, since the quality of drinking water available in the world is decreasing. Additionally, stricter wastewater discharge standards continue to be introduced worldwide, in an effort to reduce the environmental impact of industrial processes [1].

Phenol and phenol derivates used as raw materials in petrochemical and chemical industries are considered one of the most common organic water pollutants because of its high toxicity, even at low concentrations. Several technologies are available to remove industrial organic wastes, such as biological, thermal and chemical treatments and the named advanced oxidation processes (AOPs) [2–5]. Among the AOPs, the photodegradation, a technique which employs semiconductors as photocatalysts, provides a promising method for the elimination of these pollutants in water [2,6,7]. TiO_2, ZnO and SnO_2 are the semiconductor materials most widely reported as photocatalysts [8–14]. However, layered double hydroxides (LDHs) have been recently reported as a good alternative for the photodegradation of pollutant organic compounds [4]. In particular, ZnAl LDHs are successful photocatalysts for the degradation of organic compounds like methyl-orange [4], methylene blue [15] and phenol [16,17] in aqueous media.

Layered double hydroxides (LDHs) belong to a class of anionic mineral clays, with structure derived from mineral brucite, $Mg(OH)_2$. When a fraction of Mg^{2+} ions is isomorphously substituted by a trivalent ion such as Al^{3+} or Fe^{3+}, the positive charge generated on the metal hydroxide slab is compensated by the inclusion of anions generating the general formula $[M_{1-x}^{2+} M_x^{3+} (OH)_2]^{x+} (A^{n-})_{x/n}: y{\cdot}H_2O$, where M^{2+} and M^{3+} are divalent and trivalent metal ions, respectively, and A^{n-} is an intercalate anion, being CO_3^{2-} the most common [18–20]. By means of a controlled thermal decomposition, the LDHs were transformed into the respective mixed oxides.

Since ZnO [12,13] and Fe_2O_3 oxides [21,22] are well known as photocatalytically active semiconductors, in the present work the synthesis by the co-precipitation method of ZnAlFe LDHs is reported. The obtained materials were characterized by X-ray diffraction (XRD), nitrogen adsorption and UV–vis spectroscopy. The photocatalytic activity of the solids was tested towards the decomposition of the organic pollutants phenol and cresol in aqueous medium.

2. Experimental

Double layered materials containing ZnAlFe at different M_{II}/M_{III} ratio were prepared at constant pH by the co-precipitation method, using aqueous solutions of $Zn(NO_3)_2{\cdot}6H_2O$, $Al(NO_3)_3{\cdot}9H_2O$ and $Fe(NO_3)_3{\cdot}9H_2O$ (J.T. Baker Analyzed Reagent) as a source of metals. The solutions were added dropwise in a glass reactor vessel containing 800 mL of bidistilled water under vigorous magnetic stirring; the pH of the solution was adjusted to 9 by adding NH_2CONH_2 as precipitant agent. The resulting suspension was

* Corresponding author. Tel.: +52 55 58044669; fax: +52 55 58044666.
E-mail addresses: mmantillar0600@ipn.mx (A. Mantilla), fjtz@xanum.uam.mx (F. Tzompantzi).

0920-5861/$ – see front matter © 2009 Elsevier B.V. All rights reserved.
doi:10.1016/j.cattod.2009.11.006

Table 1
Molar composition Zn^{2+}/$Al^{3+}+Fe^{3+}$ and specific surface areas for the ZnAlFe calcined LDH materials.

Composition	Name	Mol Zn^{2+}/$Al^{3+}+Fe^{3+}$	Mol Al^{3+}/Fe^{3+}	BET (m^2/g)
$Zn_{1.99}Al_{2.04}Fe_{0.38}$	ZAF-5	0.824	5.42	138
$Zn_{1.27}Al_{0.90}Fe_{0.66}$	ZAF-1.5	0.814	1.36	97
$Zn_{1.99}Al_{0.802}Fe_{0.74}$	ZAF-1	1.3	1.08	79
$Zn_{2.05}Al_{0.78}Fe_{1.37}$	ZAF-0.5	0.95	0.57	117
$Zn_{3.0}Fe_{1.0}$	ZF3	3	–	83

vigorously stirred for 4 h at 363 K and maintained under reflux for 36 h. Then, the obtained materials were filtered and washed with deionized water, dried at 373 K (dried samples) for 12 h and finally, annealed at 723 K for 12 h in air flux (2 mL/s). As reference the ZnFe 3:1 oxide was prepared in similar conditions to that used for the ZnAlFe mixed oxides.

Table 1 shows the results of the final composition of the samples, which was determined by atomic absorption technique, using an analyzer model S4 (Thermo Electron Corporation). Samples were named as ZnAlFe-5, ZnAlFe-1.5, ZnAlFe-1 and ZnAlFe-0.5 for nominal Al^{3+}/Fe^{3+} ratio of 5.42, 1.36, 1.08 and 0.57, respectively. Specific surface areas of calcined samples were calculated by the BET method, using the N_2 adsorption isotherms obtained with a Quantachrome Autosorb-3B equipment.

X-ray diffraction spectra of the calcined samples were obtained with a Siemens D500 X-ray diffractometer using a graphite crystal as monochromator to select Cu-$K\alpha$ radiation (1.5406 Å) with a step of $0.02^\circ\ s^{-1}$. The band gap energy of the calcined samples was calculated from the absorption spectra obtained with a Cary 100 spectrophotometer equipped with an integration sphere.

The photodegradation of phenol in aqueous medium using the calcined samples as catalyst was carried out in a stirred Pyrex batch photoreactor; 200 ml of a solution containing 40 ppm (0.425 mmol) of phenol/g catalyst was irradiated with a UV Pen-Ray Power Supply (UVP Products) with λ = 254 nm and intensity of 4400 $\mu W/cm^2$, placed in a quartz tube, which was immersed in the solution. A series of reactors were put simultaneously under irradiation 6 h and monitored at intervals of 1 h. The same procedure was followed to determine the photodegradation of *p*-cresol, but using a solution containing 40 ppm (0.369 mmol) of *p*-cresol/g catalyst. The phenol and cresol concentration after irradiation was determined by UV–vis spectroscopy analysis, following the 269 and 275 nm absorption bands, for phenol and cresol, respectively.

3. Results and discussion

3.1. Textural properties

The specific surface areas and ZnAlFe molar ratio for the LDHs are reported in Table 1. High specific surface areas for the LDHs with different Al^{3+}/Fe^{3+} ratio were obtained, they are comprised between 138 and 70 m^2/g.

3.2. X-ray diffraction spectra

The X-ray diffraction patterns of the fresh samples showed a double layered hydroxide type structure in all the solids (Fig. 1). The peak at 11.75 in 2θ angle, corresponding to the 0 0 3 reflection of the interlayer distance in the carbonated solid, can be clearly noted. The 0 0 3 reflection is typical of hydrotalcite-type materials and its intensity is related to the crystallinity degree of the material. If a hexagonal packing is assumed, the cell parameter can be calculated by means of the 0 0 3 and 1 1 0 reflection values using the equations $c = 3d_{0\,0\,3}$ and $a = 2d_{1\,1\,0}$, where *c* corresponds

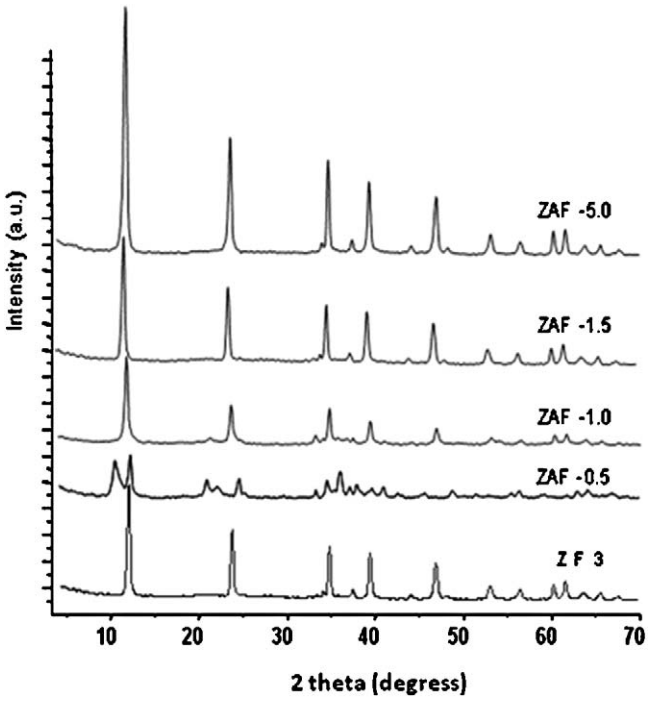

Fig. 1. X-ray diffraction patterns for LDHs with different Al/Fe ratio.

to three times the interlayer distance (0 0 3) and *a* is the average metal-metal distance in the interlayer structure (1 1 0).

The cell parameters show that the interlayer distance ($d_{0\,0\,3}$) was increased from 7.560 to 7.667 Å for the samples with the lowest and highest Fe^{3+} contents, respectively (Table 2). Additionally for the ZnAlFe-0.5 sample, a second peak with an interlayer distance of 8.878 was observed. The presence of two reflections peaks in the simple with the highest Fe^{3+} contents can be due to the intercalation of NO_3^- ions coexisting with intercalated CO_3^{2-} ions. This variation in the cell parameter could be due to the different M^{II}/M^{III} ratio in the materials, since the increasing of the positive charge could produce a higher repulsion between the material layers. LDHs can exchange the intercalated anions with different kinds of anionic molecules [23]. In order to determine the existence of some exchange between the ZnAlFe samples and phenol, the LDHs were put in contact with an aqueous solution containing 40 ppm of phenol for 6 h. The XRD spectra did not show any modification in the red parameters of the samples recovery and dried. The 11.75 2θ angle peak remains practically constant, showing the same broad and position of the peak. Thus, the intercalation of phenol in the interlayer of the ZnAlFe LDHs does not occur.

On the other hand, the XRD spectra of the samples calcined at 723 K confirms a complete destruction of the LDH structure, leading to the formation of mixed oxides (Fig. 2). In the XRD pattern, it is possible to identify the formation of zincite and hematite in which its relative abundance varies depending on the ZnAlFe composition.

Table 2
Cell parameters of the ZnAlFe LDH materials.

Catalyst	$d_{0\,0\,3}$	*c* parameter (Å)	*a* parameter (Å)
ZAF-5.0	7.5600	22.685	3.548
ZAF-1.5	7.5673	22.702	3.549
ZAF-1.0	7.5864	22.759	3.549
ZAF-0.5	8.8788	26.636	3.553
	7.6676	23.003	

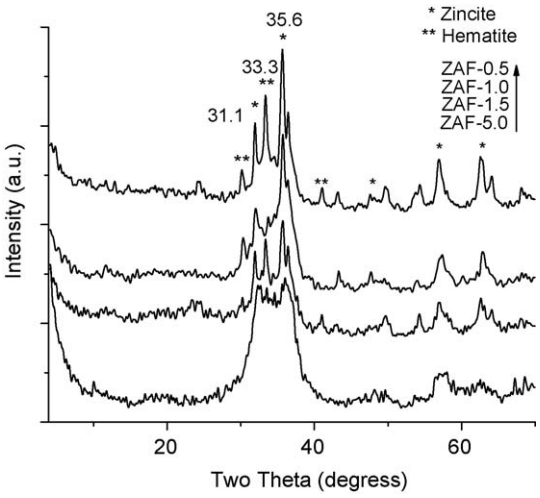

Fig. 2. X-ray diffraction spectra of ZnAlFe mixed oxides obtained after calcination at 723K.

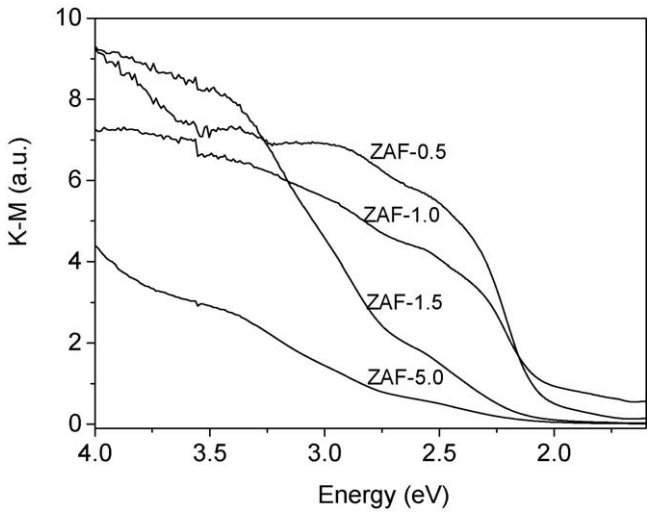

Fig. 3. UV–vis-K-M spectra for the ZnAlFe mixed oxides with different Al/Fe ratio.

3.3. Band gap energy

The evaluation of the band gap energy (E_g) for the various calcined samples was calculated using the Kubelka–Munk equation (Eq. (1))

$$F(R) = \frac{(1-R)^2}{2R} \quad (1)$$

where R is the reflectance (%) from the converted UV adsorption spectra (Fig. 3). The calculated E_g values are reported in Table 3, where it can be seen that E_g diminishes from 2.54 to 2.04 eV for the samples with the lowest and highest Fe^{3+} contents, respectively. These results show that in the mixed oxide the semiconductivity properties for the isolated Fe_2O_3 and ZnO are largely improved. The E_g band gap reported for ZnO and Fe_2O_3 are 3.2 and 2.2 eV, respectively [24].

3.4. Photodegradation study

Previous essays showed that ZAF mixed oxides are not active for the photodegradation of phenolic compounds using visible light irradiation. The inactivity showed by the mixed oxides using as irradiation source visible light, indicates that in semiconductors with low energy band gap (2.51–2.04 eV) a fast electron–hole recombination can occur giving as a result inactive photoconductors.

The evaluation of the photocatalytic activity was studied for the decomposition of phenol and *p*-cresol in liquid phase. The initial pH of the solutions for both pollutants was 7.0 and it slightly increases to 8.1 during the photodegradation.

Table 3
Band gap energy (E_g), half time and apparent first order reaction constant for the ZnAlFe mixed oxides.

Catalyst	E_g (eV)	Phenol		*p*-Cresol	
		$t_{1/2}$ (h)	K_{app}	$t_{1/2}$ (h)	K_{app}
ZAF-5.0	2.54	5.35 (7.55)	0.129 (0.091)	1.20 (4.89)	0.574 (0.141)
ZAF-1.5	2.48	4.95 (5.29)	0.139 (0.130)	1.14 (2.60)	0.607 (0.266)
ZAF-1.0	2.02	1.93 (2.62)	0.359 (0.264)	0.60 (0.96)	1.152 (0.719)
ZAF-0.5	2.04	1.01 (1.93)	0.683 (0.357)	0.59 (0.73)	1.164 (0.943)
TiO_2-P25	3.01	1.16	0.597	1.182	0.586

The value in the parenthesis corresponds to the photocatalytic test for used photocatalysts.

In order to determine if phenol can be directly photolyzed by UV light the phenolic solution without catalyst was irradiated and the results are showed in Fig. 4, where a slight increase in the UV spectra lecture $C/C_0 > 1.0$ can be seen. This phenomenon may be due to some kind of modification suffered by the compound, which increases the absorbance at 269 nm. Therefore, and according to these results, it is reasonable to assume that phenol is not photolyzed by UV light at 254 nm.

The pollutant disappearance as a function of time was followed by the UV analysis of aliquots form the irradiated solution at different time intervals, Fig. 4 shows that the phenol photodegradation activity is, in fact, a function of the Fe^{3+} content in the samples. The higher activity was obtained on the sample with lower Al/Fe ratio. The effect of the Fe^{3+} content in the phenol degradation is quite important, since the phenol practically disappears (98%) after 6 h of irradiation with the ZnAlFe-0.5 sample, while for the ZnAlFe-5 and ZnAlFe-1.5 semiconductors the phenol degradation values were 50 and 48%, respectively. It must be noted that the ZF3 sample shoes if any a very low activity.

The phenol photodegradation follows a pseudo-first-order kinetic and the rate constant was evaluated from Fig. 5; the

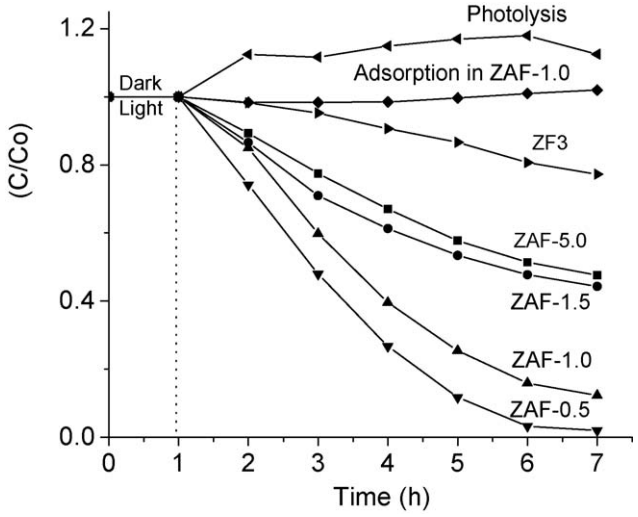

Fig. 4. Photodegradation of phenol (40 ppm) in aqueous solution for ZnAlFe mixed oxides with different Al/Fe ratio.

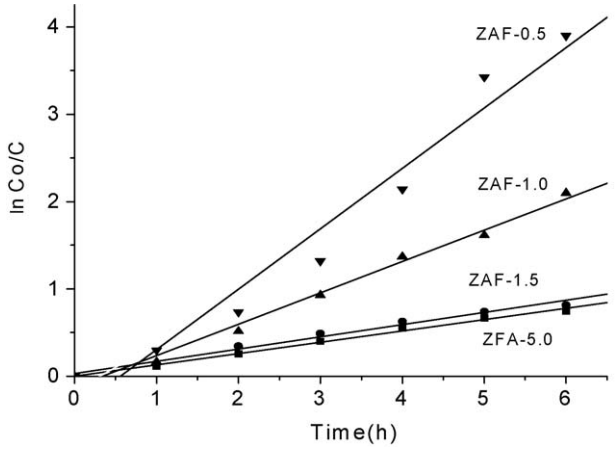

Fig. 5. Pseudo-first-order kinetic for the photodegradation of phenol for ZnAlFe mixed oxides with different Al/Fe ratio.

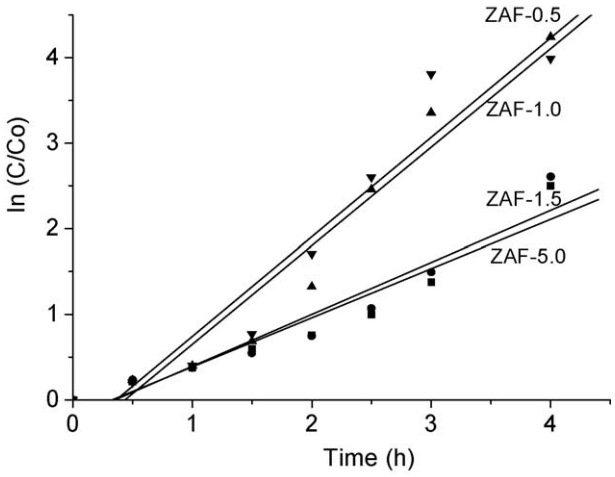

Fig. 7. Pseudo-first-order kinetic for the photodegradation of *p*-cresol for ZnAlFe mixed oxides with different Al/Fe ratio.

results in Table 3 are reported as $t_{1/2}$, which is the required time to decompose half of the phenol present in the irradiated solution.

The *p*-cresol photodecomposition was also evaluated in the ZnAlFe mixed oxides and Fig. 6 shows the results as a function of time for the various semiconductors. As it was discussed for phenol it is reasonable to assume the same explanation for the photolysis phenomenon observed in *p*-cresol $C/C_0 > 1.0$. Similar behavior to that presented on the phenol photodegradation can be observed: i.e., the more active photocatalysts are those with the highest content of Fe^{3+}; however, in this case the total *p*-cresol photodegradation was reached after only 4 h of irradiation with the ZnAlFe-1.0 and ZnAlFe-0.5 photocatalysts. Note that the reference ZF-3 showed a very low photoactivity. As for the case of phenol photodegradation, the reaction rate follows a pseudo-first-order and the plot of $\ln C/C_0$ vs time allows for the calculation of the reaction constant and $t_{1/2}$ (Fig. 7). According to the results reported in Table 3, it can be seen that the *p*-cresol photodegradation occurs faster than phenol photodegradation. For both reactions the presence of a high number of intermediates of the photodegradation with TiO_2 as photocatalyst has been reported by several authors: pyrocatechol and hydroquinone have been detected as hydroxylated products of phenol, which degrade rapidly via fumaric acid, organic acids and to CO_2 [25] and *o*-hydroxy benzyl alcohol or hydroxy benzoic acid for cresol [26]. However, in our knowledge any report has been made for phenol and *p*-cresol photodegradation with ZnAlFe mixed oxides derived from LDHs; the identification of the possible intermediate compounds was attempted by analyzing by GC (Perkin Elmer Autosystem XL, column Quadrex 007 FFAP) the irradiated aqueous solutions containing the ZAF-0.5 catalyst. The analysis showed that any of the intermediates previously mentioned were detected. Thus, the photodegradation almost is conducted until reach a total mineralization of the phenolic compounds. In order to prove this assumption, the total organic compounds (TOC) analysis as a function of the time was carried out for phenol and *p*-cresol photodecomposition using a TOC analyzer (Shimadzu TOC-V CSP) and the results are reported in Figs. 8 and 9 respectively. A mineralization >98% can be observed with the ZAF-0.5 and ZAF-1.0 catalysts after 6 h for the phenol and *p*-cresol photodegradation. These results show unlike the titania photocatalysts behavior, the total mineralization of phenolic compounds can be achieved by using ZnAlFe mixed oxides obtained from DLHs type precursors. In order to study their stability, the mixed oxides they were dried, reactivated at 350 °C and proved under identical work conditions. The results reported in Table 3, showed that from the catalysts evaluated, the most stables are those with the lower Fe_2O_3 content;

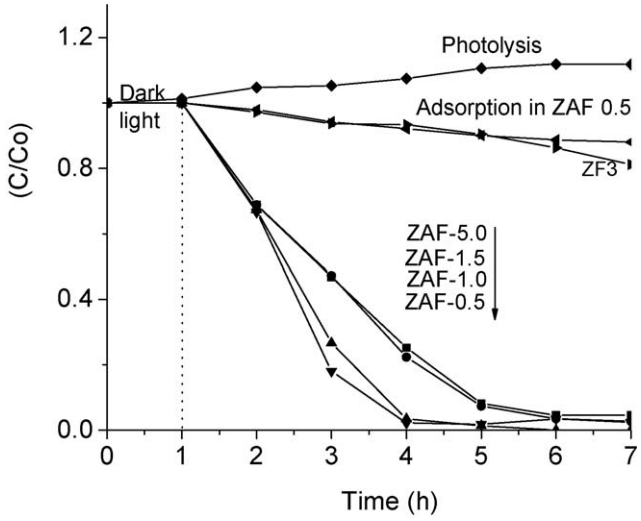

Fig. 6. Photodegradation of *p*-cresol (40 ppm) in aqueous solution for ZnAlFe mixed oxides with different Al/Fe ratio.

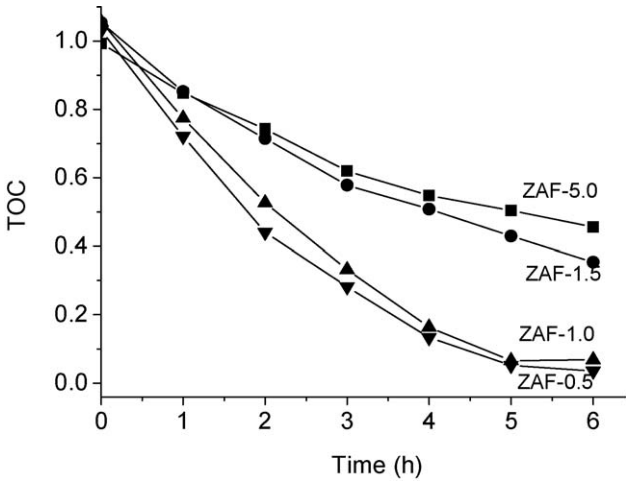

Fig. 8. TOC as a function of the time for the photocatalytic degradation of phenol on ZnAlFe mixed oxides with different Al/Fe ratio.

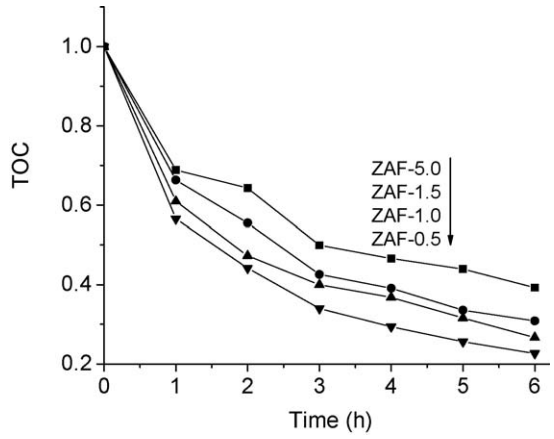

Fig. 9. TOC as a function of the time for the photocatalytic degradation of *p*-cresol on ZnAlFe mixed oxides with different Al/Fe ratio.

i.e. they are less active but in contrast they are more resistant to deactivation. In order to show the high efficiency for the photocatalytic decomposition of the phenolic compounds, comparative results were obtained by using the well known titania Degussa-P25 commercial catalyst (inserted in Table 3). For the phenol decomposition the ZAF-0.5 and P-25 catalysts showed a comparable photoactivity with $t_{1/2}$ values of 1.01 and 1.16 h respectively. In the case of the *p*-cresol photodegradation the ZAF-0.5 photoactivity value ($t_{1/2}$ = 0.595 h) was twice than those obtained for P-25 ($t_{1/2}$ = 1.18 h).

The present work show that ZnAlFe mixed oxides prepared from their corresponding LDHs crystalline structure are promising photocatalysts for the decomposition of phenolic compounds in aqueous medium. In addition economic benefits can be obtained, since low price soluble nitrates were used as starting precursors for the synthesis of these materials.

4. Conclusions

The results of the present work show the successful synthesis of ZnAlFe layered double hydroxides from soluble salts with LDHs crystalline structures in all of the samples. After calcination at 723 K, the LDHs crystalline structure was destroyed and the respective mixed oxides were obtained. The obtained mixed oxides show high specific surface areas and important semiconductor properties, with E_g band gaps of 2.54–2.04 eV. With respect to the photodegradation of phenol, high degradation values (98%) was reached with the ZnAlFe-0.5 catalyst, after 6 h of irradiation; a total degradation of cresol was obtained at only 4 h of irradiation with ZnAlFe-0.5 and ZnAlFe-1 catalysts and after 6 h with ZnAlFe-1.5 and ZnAlFe-5.

Acknowledgments

We are indebted to SEP-CONACYT for the support provided to the CB-2006-1-62053 research project. A. Mantilla thanks CONACYT for scholarship support.

References

[1] L.F. Liotta, J. Hazard. Mater. 162 (2009) 588.
[2] N. Hadj Salah, M. Bouhelassa, S. Bekkouche, A. Boultif, Desalination 166 (2004) 347;
G. Busca, S. Berardinelli, C. Resini, L. Arrighi, J. Hazard. Mater. 160 (2008) 265.
[3] S. Esplugas, J. Gimenez, S. Contreras, E. Pascual, M. Rodriguez, Water Res. 36 (2002) 1034.
[4] E.M. Seftel, E. Popovici, M. Mertens, K. De Witte, G. Van Tendeloo, P. Cool, E.F. Vansant, Micropor. Mesopor. Mater. 113 (2008) 296.
[5] E. Regina, L. Tiburtius, P. Peralta-Zamora, A. Emmel, J. Hazard. Mater. B 126 (2005) 86.
[6] M.A. Rauf, S.S. Ashraf, Chem. Eng. J. (2009), doi:10.1016/j.cej.2009.02.026.
[7] A. Vaccari, Catal. Today 41 (1998) 53.
[8] S. Lathasree, A.N. Rao, B. SivaSankar, V. Sadasivam, K. Rengaraj, J. Mol. Catal. A: Chem. 223 (2004) 101.
[9] J. Saien, H. Nejati, J. Hazard. Mater. 148 (2007) 491.
[10] F. Han, V.S.R. Kambala, M. Srinivasan, D. Rajarathnam, R. Naidu, Appl. Catal. A: Gen. 359 (2009) 25.
[11] U.I. Gaya, A.H. Abdullah, J. Photochem. Photobiol. C: Photochem. Rev. 9 (2008) 1.
[12] S.K. Pardeshi, Solar Energy 82 (2008) 700.
[13] E. Evgenidou, I. Konstantinou, K. Fytianos, I. Poulios, T. Albanis, Catal. Today 124 (2007) 156.
[14] C. Wang, B.-Q. Xua, X. Wang, J. Zhao, J. Solid State Chem. 178 (2005) 3500.
[15] M. Parida, N. Baliarsingh, B. Sairam Patra, J. Das, J. Mol. Catal. A: Chem. 267 (2007) 202.
[16] R. Kun, M. Balázs, I. Dékány, Coll. Surf. A: Physicochem. Eng. Aspects 265 (2005) 155.
[17] A. Patzko, R. Kun, V. Hornok, I. Dekany, T. Engelhardt, N. Schall, Colloids Surf A: Physicochem. Eng. Aspects 265 (2005) 64.
[18] F. Cavani, F. Trifiro, A. Vaccari, Catal. Today 11 (1991) 173.
[19] S. Miyata, Clays Clay Miner. 23 (1975) 369.
[20] A. De Roy, C. Forano, K. ElMalki, J.P. Besse, Synthesis of microporous materials, in: M.L. Occelli, H.E. Robson (Eds.), Expanded Clays and Other Microporous Systems, vol. 2, Van Nostrand Reinhold, New York, 1992 (Chapter 7).
[21] R. Liou, S. Chen, M. Hung, C. Hsu, J. Lai, Chemosphere 59 (2005) 117.
[22] M. Noorjahan, V. Durga Kumari, M. Subrahmanyam, L. Panda, Appl. Catal. B: Environ. 57 (2005) 291.
[23] K.H. Goh, T.-t. Lim, Z. Dong, Water Res. 42 (2008) 1343.
[24] C. Karunakaran, R. Dhanalakshmi, Solar Energy Mater. Solar Cells 92 (2008) 1315.
[25] H. Chun, W. Yizhong, T. Hongxiao, Chemosphere 41 (2000) 1205.
[26] B. Pal Hata, K. Goto, G. Nogami, J. Mol. Catal. A: Chem. 169 (2001) 147.